Bioresource Technology 406 (2024) 130967

Contents lists available at ScienceDirect

Bioresource Technology

journal homepage: www.elsevier.com/locate/biortech

Robust, fully quantifiable and scalable bioprocess utilizing spent sulfite liquor with *Corynebacterium glutamicum*

Daniel Waldschitz [a], Mark-Richard Neudert [a], Jakob Kitzmueller [a], Johanna Lachmann [a], Arthur Fonteyne [b], Karolien Maes [b], Nadav Bar [c], Peter Sinner [a], Oliver Spadiut [a,*]

[a] Research Group Bioprocess Technology, Institute of Chemical, Environmental and Bioscience Engineering, TU Wien, Gumpendorferstraße 1A, Vienna A-1060, Austria
[b] Bio Base Europe Pilot Plant vzw, Rodenhuizekaai 1, Gent B-9042, Belgium
[c] Department of Chemical Engineering, Faculty of Natural Sciences, NTNU, Sem Sælands vei 6, Trondheim N-7491, Norway

HIGHLIGHTS

- Minimal medium for *C. glutamicum* based on ultra-filtrated spent sulfite liquor.
- Biomass quantification with high water insoluble solids via tryptophan fluorescence.
- Comprehensive quantification via elemental balances of highly complex system.
- Identification of batch kinetics using monod like mechanistic model.
- Successful scale-up from 3 L *lab-scale* to 150 L *pilot-scale*.

GRAPHICAL ABSTRACT

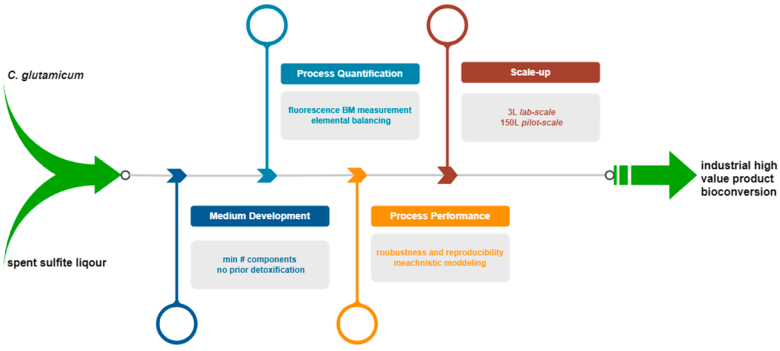

ARTICLE INFO

Keywords:
Lignocellulosic feedstock
Minimal medium
Fluorescence biomass measurement
Fermentation
Scale-up

ABSTRACT

In this study, a bioprocessing strategy was designed to valorize ultra-filtered spent sulfite liquor (UF-SSL) without prior detoxification steps as well as using it purely as a carbon source supplement to defined or complex media. Hence, a minimal medium for the bioconversion of UF-SSL with *Corynebacterium glutamicum* was developed and process robustness and reproducibility were validated. Process quantifiability was ensured by development of a biomass measurement technique for matrices with high water-insoluble solids and verified using elemental balancing. Mechanistic modeling based on Monod equations was used to identify batch kinetics. In a final step, scale-up of the developed process was performed to showcase process maturity towards commercialisation.

1. Introduction

The development of bioprocesses based on 2nd generation renewable resources is being promoted and prioritized by regulatory authorities, such as the European Union, due to their contribution to the reduction of greenhouse gas emissions and the establishment of a circular economy (de Jong et al., 2012). Among these, agro-forestry residues and their respective processing side-streams have been identified as feedstocks

* Corresponding author.
E-mail address: oliver.spadiut@tuwien.ac.at (O. Spadiut).

https://doi.org/10.1016/j.biortech.2024.130967
Received 25 April 2024; Received in revised form 2 June 2024; Accepted 11 June 2024
Available online 14 June 2024

with the greatest potential for renewable bioprocessing due to their low cost, high abundance, and compliance with environmental sustainability goals (Hassan et al., 2019). One resource which combines multiple benefits for renewable and sustainable production of 2nd generation bioproducts is spent sulfite liquor (SSL), a side stream from the pulp and paper industry (Rueda et al., 2015). Key advantages of SSL include its high year-round availability, low cost, and high abundance. In addition, the pulping process acts as a pretreatment resulting in a high fraction of fermentable sugars and allows for the possibility of integration into existing biorefinery-based pulp and paper mills. Existing biorefineries based on SSL are mainly focused on the production of low-value ethanol (Rødsrud et al., 2012). However, the production of high-value products is a key factor for improving the economic viability of biorefineries (de Jong et al., 2012). SSL poses several challenges as a substrate for biomass growth as it is a complex mixture of various C5 and C6 sugars, organic acids, such as acetate, inhibitory compounds, such as furfural and 5-hydroxymethylfurfural (HMF), and phenolic compounds from lignin degradation (Fatehi and Ni, 2011). Therefore, existing processes often rely on additional pretreatment steps to detoxify the substrate SSL, such as boiling (Nigam, 2001) and overliming (Guo and Olsson, 2014), and/or using the SSL as a carbon source supplement in existing defined (Pereira et al., 2015) or complex (Brandt et al., 2022) media, which increases production costs. Current ethanol production processes primarily use yeasts, such as *Saccharomyces cerevisiae* species (Rødsrud et al., 2012). By diversifying the host organisms for the bioconversion of SSL, the catalog of high value products available from 2^{nd} generation agro-forestry resources can be expanded.

In this study, a bioprocessing strategy without existing complex or defined media and detoxification pretreatment steps was developed for a novel ultra-filtered spent sulfite liquor (UF-SSL) bioconversion host. In recent years, *Corynebacterium glutamicum* has been identified as a promising host for this purpose due to its natural ability to degrade inhibitory substances, such as aromatic compounds (Shen et al., 2012), acetate (Kiefer et al., 2021) and furfural (Tsuge et al., 2016), as well as its universal resistance mechanism based on mycothiol (Liu et al., 2013), which increases its general robustness to a wide variety of chemicals. In addition, *C. glutamicum* has been extensively genetically modified to utilize a wide variety of carbon sources as well as to produce high-value products (Becker et al., 2018). To date, *C. glutamicum* has only been cultivated on defined media supplemented with UF-SSL as a carbon source in *lab-scale* by Sinner et al. (2021). To improve the economic feasibility of bioprocesses using *C. glutamicum* grown on UF-SSL, the objectives of this study were to develop a minimal medium for *C. glutamicum* by adding only essential components to UF-SSL while allowing robust and reproducible growth. Furthermore, process quantifiability should be ensured by using a novel biomass measurement for background matrices with high water-insoluble solids (WIS) and validation thereof by rigorous elemental balancing. Subsequently, batch kinetics were identified through Monod-like mechanistic modeling. Ultimately, scaling-up the developed process from *lab-scale* to *pilot-scale* should be performed to demonstrate process maturity.

2. Materials and methods

2.1. Raw material and strain

The low molecular weight permeate of ultra-filtered spent sulfite liquor (UF-SSL) from softwood pulping (stored at 4°C) was used for all experiments. For this study, *Corynebacterium glutamicum* CR099::U pXMJ19 was used (Cao et al., 2024). Similar strains with an improved uptake of mannose and the capability to metabolize xylose, such as *C. glutamicum* ATCC 13032 pVWEx1-manA pEKEx3-xylAB, had the sugar utilization genes encoded on plasmids and were tested on full defined cultivation medium plus UF-SSL (Sinner et al., 2021). The present strain carried the sugar metabolization genes directly in the genome (denominated by ::U), making way for integration of plasmids encoding for product biosynthesis genes, and thus converting the strain into a suitable chassis for production purposes on SSL.

2.2. Experimental setup

Preculture. Cells were stored at −80 °C and streaked out onto 2TY-agar plates [16 g/L tryptone, 10 g/L yeast extract, 5 g/L NaCl, 10 g/L agar, heat sterilized, 12 mg/L chloramphenicol] and incubated [48 h, 30 °C]. Afterwards, single colonies were used to inoculate 12.5 ml 2TY liquid medium (same composition as before but without agar) in 50 ml reaction tubes and incubated [30 °C, 230 rpm, 24 h] as seed 1. Subsequently, seed 1 was transferred into 1L shake flasks with 225 ml 2TY medium and 25 ml SSL-MOPS [100 v/v% UF-SSL, 100 g/L 3-(N-morpholino) propanesulfonic acid (MOPS), pH 7, sterile filtered] and incubated [30 °C, 230 rpm, 18 h] as seed 2. For inoculation of the bioreactor, seed 2 was harvested by centrifugation in 50 ml reaction tubes [3420 RCF, 4 °C, 5 min] and resuspended in saline solution [0.9 g/L NaCl, heat sterilized] and 75 ml inoculum were transferred by syringe.

Bioreactor cultivation. Lab-scale bioreactors (Labfors 5, Infors, Germany) with 3 L working volume glass vessels equipped with optical dO2 probes (Visferm DO, Hamilton, Switzerland), potentiometric pH probes (Easyferm PHI, Hamilton, Switzerland) as well as off-gas analyzers (BlueInOne Ferm, BlueSense, Germany) were used. pH was controlled at a level of 7.00 +/- 0.02 via the addition of 2.5 M KOH and 2.5 M H_2SO_4. dO2 was controlled at 30 % by increasing the agitator speed (400–1200 rpm) at a constant air flow of 0.3 vvm. Temperature was maintained at 30 °C throughout the cultivation. The batch media consisted of UF-SSL diluted respectively as indicated for each experiment, sterile filtered (0.2 μm) and supplemented [0.2 mg/L biotin, 12 mg/L chloramphenicol, 5 ml/L polyproylenglycol 2000] with a starting volume of 1 L. The nitrogen and phosphorus (NP) feed [66.4 g/L urea and 71.8 g/L KH_2PO_4, sterile filtered] was supplied during the cultivation ($\dot{V} = 4.5$ mL/h until 100 ml were fed). Data was collected using a process information management system (PIMS) (Lucullus, SecureCell, Switzerland) and process control was performed using MATLAB (MATLAB2021b, Mathworks, USA) via the Rest-API interface of the PIMS. Samples were collected every 3 h using an automated sampling device (custom-built by the research group) and stored at 4 °C until further analysis.

Scale-up was performed at a commercial pilot plant (BBEPP, Ghent, Belgium) in 150 L stainless steel bioreactors (Custom Design, Frings, Germany) with a starting volume of 40 L and sampling performed manually. Inoculum quantitiy, UF-SSL dilution, NP feed concentration and feed rate were adjusted to ensure maximum comparability of nutrient availability between scales. To ensure constant kLA between scales, dO2 was controlled at 30 % by increasing the agitator speed (115–600 rpm, 0.96–5 m/s) at a constant air flow of 0.3 vvm and 500 mbar.

2.3. Analytical methods

Biomass measurement development. A calibration set of 42 samples of cells grown on 2TY medium was prepared according to Section 2.2 without UF-SSL. Cells were harvested by centrifugation [3420 RCF, 4°C, 5 min] and re-suspended in with saline solution (0.9% NaCl) twice to remove matrix components. A serial dilution on 96-well plates (PP black, Microplate, 96-well, F-Bottom; Grainer BIO-ONE) of all samples with saline solution was prepared by adding 100 μl saline to all wells and 100 μl sample into the first row. Subsequently, the serial dilution was performed using a multichannel pipette by mixing the current well by pipetting up and down 4 times and transferring 100 μl to the next row. Before entering the last row of the 96-well plate, the remaining 100 μl were discarded in order to reserve the last row as blank, leaving 100 μl liquid were left in each well. Fluorescence (EX:280/15 nm; EM:340/20 nm) was measured using a plate reader (Spark, Tecan, Switzerland). A validation set of 24 samples was prepared analogous to the calibration

set, with one part was used for measurement of cell dry weight (1.8 ml, 14000 RCF, 10 min followed by removal of the supernatant and drying at 72 °C, 3 days) and the second part for measurement of fluorescence.

Further analytes. Sugars and urea were quantified using high pressure liquid chromatography (HPLC) (UltiMate U3000, ThermoFischer, USA) from filtered supernatants (0.2 μm), using a Pb-column (Nucleogel Sugar Pb 300 mm, Macherey–Nagel, Germany) with an isocratic flow of ultrapure water (0.4 ml/min, 79°C), equipped with an RI detector (RI-100, Shodex, USA). Organic acids, ammonia and phosphate were quantified from the supernatant using automated enzymatic photometric assays (CEDEX Bio HT Analyzer, Roche, Switzerland). For measurement of dry mass, samples were first centrifuged [3420 RCF, 4°C, 5 min] in predryed 2 ml reaction tubes, the supernatant was removed and the reaction tubes were dried [72°C, 3 d] before gravimetric determination.

2.4. Data analysis

Data evaluation was performed in MATLAB (MATLAB 2021b, Mathworks, USA). The model was adapted from Sinner et al. (2021) by the addition of a fourth substrate (acetate) as well as the remodelling of substrate interactions. Rate calculation, model parameterization and validation were performed as described by Sinner et al. (2019) (for more detail on the modelling procedure readers are referred there). In addition, the change in reactor volume (V_R) was calculated as the total volumetric influx ($\dot{V}_{in}$) by the addition of acid, base and NP feed.

$$\frac{dV_R}{dt} = \dot{V}_{in} \tag{1}$$

Substrate uptake rates (q_{S_i}) were modeled monod like for glucose (S_1), mannose (S_2), xylose (S_3) and acetate (S_4), with competitive inhibition by glucose on mannose and xylose uptake.

$$q_{S_1} = q_{S_1,max} \cdot \frac{S_1}{S_1 + K_{S_1}} \tag{2}$$

$$q_{S_2} = q_{S_2,max} \cdot \frac{S_2}{S_2 + \frac{K_{S_2}}{K_{S_1}} \cdot S_1 + K_{S_2}} \tag{3}$$

$$q_{S_3} = q_{S_3,max} \cdot \frac{S_3}{S_3 + \frac{K_{S_3}}{K_{S_1}} \cdot S_1 + K_{S_3}} \tag{4}$$

$$q_{S_4} = q_{S_4,max} \cdot \frac{S_4}{S_4 + K_{S_4}} \tag{5}$$

$$\frac{dS_i}{dt} = q_{S_i} \cdot X - S_i \cdot \frac{\dot{V}_{in}}{V_R} \tag{6}$$

Biomass (X) production was modeled as the sum of substrate uptake rates (q_{S_i}) times their respective yield coefficients (Y_{X/S_i}).

$$q_X = q_{S_1} \cdot Y_{X/S_1} + q_{S_2} \cdot Y_{X/S_2} + q_{S_3} \cdot Y_{X/S_3} + q_{S_4} \cdot Y_{X/S_4} \tag{7}$$

$$\frac{dX}{dt} = q_X \cdot X - \frac{\dot{V}_{in}}{V_R} \cdot X \tag{8}$$

Carbon dioxide evolution rate (CER) and oxygen uptake rate (OUR) were modeled based on first-principle elemental and degree of reduction (DOR) balances.

$$CER = X \cdot V_R \cdot \sum q_{S_i} \cdot \left(\frac{1}{M_{C_{mol}S_i}} - \frac{Y_{X/S_i}}{M_{C_{mol}X}} \right) \tag{9}$$

$$OUR = \frac{X \cdot V_R}{DOR_{O_2}} \cdot \sum q_{S_i} \cdot \left(\frac{DOR_{S_i}}{M_{C_{mol}S_i}} - \frac{Y_{X/S_i} \cdot DOR_X}{M_{C_{mol}X}} \right) \tag{10}$$

Biomass composition $\left[M_{C_{mol}X} = 27.78 g/C_{mol};\ DOR_X = 4.18 e^-_{mol}/C_{mol}\right]$ was taken from Sinner et al. (2021) and molecular constants were calculated $\left[M_{C_{mol}S_{1,2,3}} = 30.03 g/C_{mol};\ M_{C_{mol}S_4} = 29.52 g/C_{mol};\ DOR_{O_2} = -4.0 e^-_{mol}/C_{mol};\ DOR_{S_{1,2,3,4}} = 4.0 e^-_{mol}/C_{mol}\right]$.

3. Results and discussion

3.1. Minimal medium development

As a first step towards the development of an industrially relevant minimal medium, the composition of UF-SSL was analyzed and compared to a standard medium for *C. glutamicum* CGXII, first described by Keilhauer et al. (1993), to see which nutrients are already present in UF-SSL and to avoid unnecessary addition of nutrients (Table A.1). Compared to the defined medium CGXII, which is based on glucose as the sole carbon source, UF-SSL contained a variety of sugars and organic acids, which can be utilized by different organisms to varying degrees. However, CGXII and UF-SSL contained similar amounts of glucose, which is the primary carbon source used by most heterotrophic microorganisms. In contrast to carbon, the bioavailable amounts of nitrogen and phosphate in the UF-SSL were significantly lower than in CGXII. Trace element concentrations in UF-SSL were comparable to or exceeded those added to CGXII, with the exception of copper. Copper exerts significant toxicity on trees, resulting in a reported average concentration of only 10 µg/g dry weight in plant tissue (Yruela, 2005). Considering that SSL is derived from plant tissue, copper concentrations below the detection limit in UF-SSL are not surprising. Furthermore, the vitamin biotin, for which *C. glutamicum* is auxotrophic, as well as the growth enhancing component protocatechuic acid (Unthan et al., 2014) were not measured for UF-SSL. Similarly, buffer components, antibiotics, and antifoam were not considered to be present in UF-SSL. In summary, while all trace elements (with the exception of copper) were present at similar or higher quantities (per gram of the primary carbon source glucose) in UF-SSL than in CGXII, sources of bioavailable nitrogen, phosphate, and biotin were lacking. Therefore, to use UF-SSL as an industrial cultivation medium, separate sources of these components must be added, while UF-SSL can supply the carbon and trace elements necessary for growth.

To minimize the cost of the minimal medium for industrial production, the number of added components should be minimized. Therefore, only one source of N and P was taken from the two originally present in CGXII. Urea was chosen as the N source since it is reported to be viable as a sole nitrogen source for *C. glutamicum* and superior to ammonium sulfate in terms of protein expression (Morschett et al., 2020). As an added benefit, unlike ammonia, urea does not have the tendency to be stripped from the liquid phase by evaporation. The P sources used in the CGXII are KH_2PO_4 and K_2HPO_4. However, since the phosphate buffer system is not required in a pH-controlled bioreactor, only KH_2PO_4 was selected as phosphorus source and the buffer component MOPS was completely omitted. Although the presence of biotin in extracts of lignocellulosic biomass was reported by Han et al. (2019), initial tests showed that biomass growth was $\simeq$ 50 % in cultivations without added biotin compared to cultivations with the same concentration as present in CGXII spiked into the SSL (data not shown). Therefore, biotin was added to the UF-SSL at the same concentration as in CGXII to ensure growth. Protocatechuic acid, which is used to further enhance biomass growth in defined medium, was omitted due to cost (Unthan et al., 2014). The addition of potassium phosphate directly to UF-SSL resulted in the formation of a precipitate. Due to the large quantities of calcium present in the UF-SSL, the formation of calcium phosphate was established as a working hypothesis. Since the precipitate did not dissolve as the concentration of PO_4 in solution decreased, the P in the precipitate was no longer considered bioavailable and thus lost for cell growth. To counteract and overcome these challenges, a separate nitrogen and phosphate feed (NP-Feed) was utilised in order to i) ensure consistent supply of N and P for cell growth and ii) minimize the precipitation of P

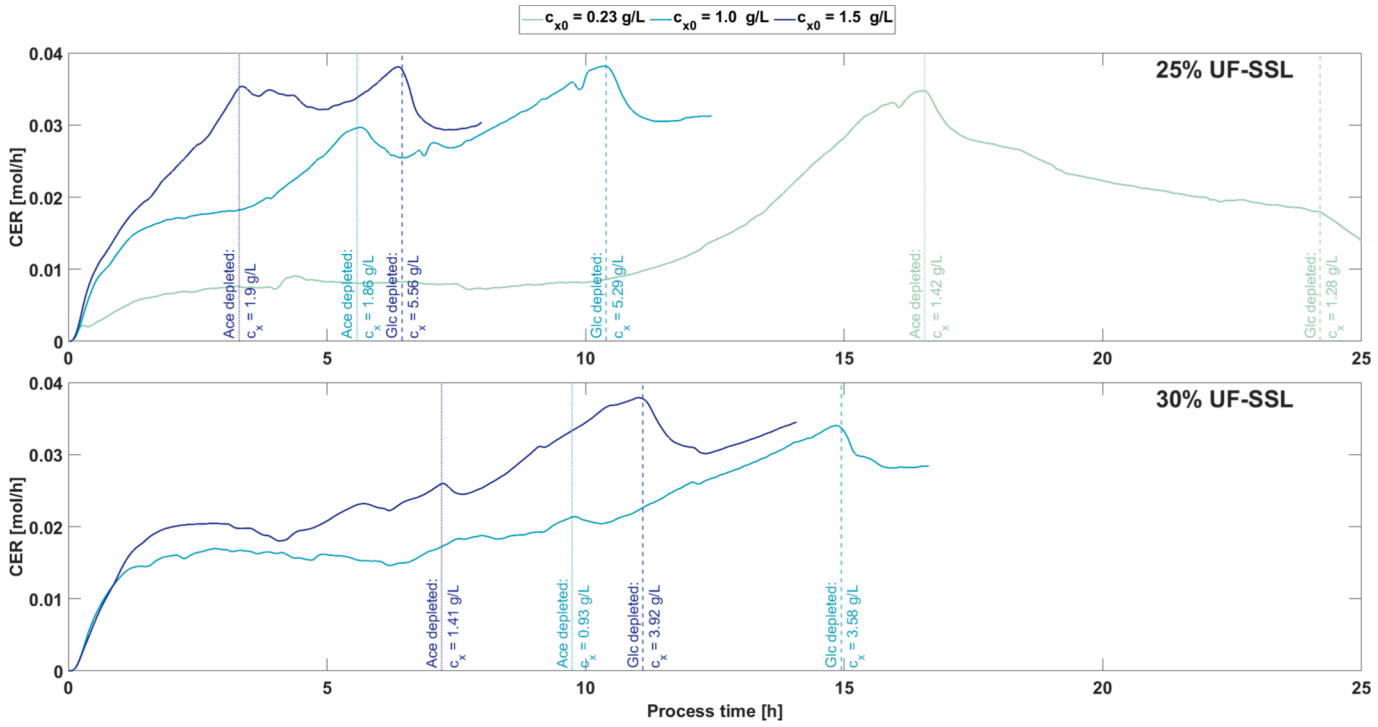

Fig. A.1. Effect of different UF-SSL concentrations and initial biomass concentrations on the cultivation. A ≃ 16 h long lag phase is observed in the CER for 25 % UF-SSL (top) when starting with 0.23 g/L initial biomass. Increasing the starting biomass concentration decreased the lag phase but with diminishing returns for increasing the biomass per substrate yield. The same effect occured at 30 % UF-SSL (bottom), although the initial biomass concentration needed to be higher in order to compensate for the increased inhibitor concentrations.

and evaporation of N by keeping the dissolved concentrations at low levels. While the maximum availability of PO_4 was determined by its solubility in UF-SSL (≃ 5 mmol/L at pH 7), PO_4 addition had to be balanced to replace consumed PO_4, by keeping the measured PO_4 concentration in solution constant. For N on the other hand, Kiefer et al. (2021) reported the optimal molar ratio between C and N for *C. glutamicum* batch growth on lignocellulosic acetate with ammonia to be 10/1. Hence, this molar ratio was used and adapted with lignocellulosic UF-SSL and urea.

In order to properly verify the growth of *C. glutamicum* on the proposed medium, a suitable NP addition strategy as well as process starting conditions had to be selected. An exponential feeding profile for NP which scales with biomass growth, as is typical for fed-batch processes, would have resulted in very low feed rates at the beginning of the batch due to the low biomass concentration at inoculation. Low feeding rates were considered error prone and therefore undesirable. Similarly, diluting the feed to achieve higher pumping rates would have resulted in unnecessary volume being added to the reactor. Hence, a linear NP-Feed was tested during the batch for supply of nitrogen and phosphate. Due to the presence of inhibitors, such as furfural and HMF, the cells entered a lag phase upon exposure, resulting in a longer batch phase and decreased biomass to substrate yields (van Dijk et al., 2019). During the lag phase, the cells degraded inhibitors before starting their growth, thus the length and severity of the lag phase was determined by the initial biomass to inhibitor ratio. In addition to the time spent waiting for the lag phase to end, its occurrence also coincided with a decrease in substrate to biomass yields. Therefore, the adaptation and lag phases of the cells should be kept as short as possible to increase both space–time and substrate to biomass yields. In order to overcome inhibitor-related challenges to build a robust bioconversion process, Xiros and Olsson (2014) outlined 4 key strategies: inhibitor reduction (pretreatment, detoxification), improved strain performance (strain engineering, short-term adaptation), optimized fermentation conditions (nutrients, inoculum size) as well as process design (optimization of process schemes, process modes). The desired process design was a batch phase, and SSL (considering the pulping process as a pretreatment for the production of fermentable sugars) had a higher concentration of inhibitors than softer enzymatic or dilute acid hydrolysates. Their removal may be economically disadvantageous due to increased cost and process complexity, leaving the strain performance and process conditions to be optimized. As inhibitor presence for *C. glutamicum* was reported to lead to decreased growth while metabolic activity was reported to be significantly less affected than for other host organisms (Sakai et al., 2007), direct degradation of the inhibitors by the cells might be more economical. To perform a short-term adaptation (Tomás-Pejó and Olsson, 2015) and thus pre-adapt the cell to the presence of SSL, 10 %(v/v) UF-SSL were added to the 2TY medium in the final pre-culture step before inoculation (data not shown). Furthermore, the main options to reduce the lag phase and biomass per substrate yields are the dilution of SSL used and the initial biomass concentration at inoculation. Therefore, various dilutions of UF-SSL and initial biomass concentrations were tested for batch optimization. As an additional consideration, the amount of C source present at the start of the batch affects whether overflow metabolism occurs, which would also reduce the yield of substrate to biomass. Typical starting glucose concentrations for the batch phase on defined media range from 5 to 15 g/L, with 10 g/L being most common. Therefore, similar initial glucose concentrations were targeted for SSL, resulting in UF-SSL dilutions of 25–30 %(v/v) with water.

The carbon dioxide evolution rate (CER) can be used to track at which time-point certain substrates are depleted (Fig. A.1). During a severe lag phase, after an initial increase in CO_2 upon inoculation, a flattening CER was observed. During this study, lag phases ranging from ⩽1 h up to ⩾24 h were observed. Acetate was the first C source to be depleted by *C. glutamicum* in UF-SSL, which coincided with a small peak in the CER, followed by a bigger bump ≃ 5 h later, when glucose was depleted. Raising the target biomass concentration for inoculation had a positive effect on the lag phase and substrate to biomass yields. A typical target starting optical density for *C. glutamicum* is $OD_{600} = 1$ (≃ 0.23 g/L

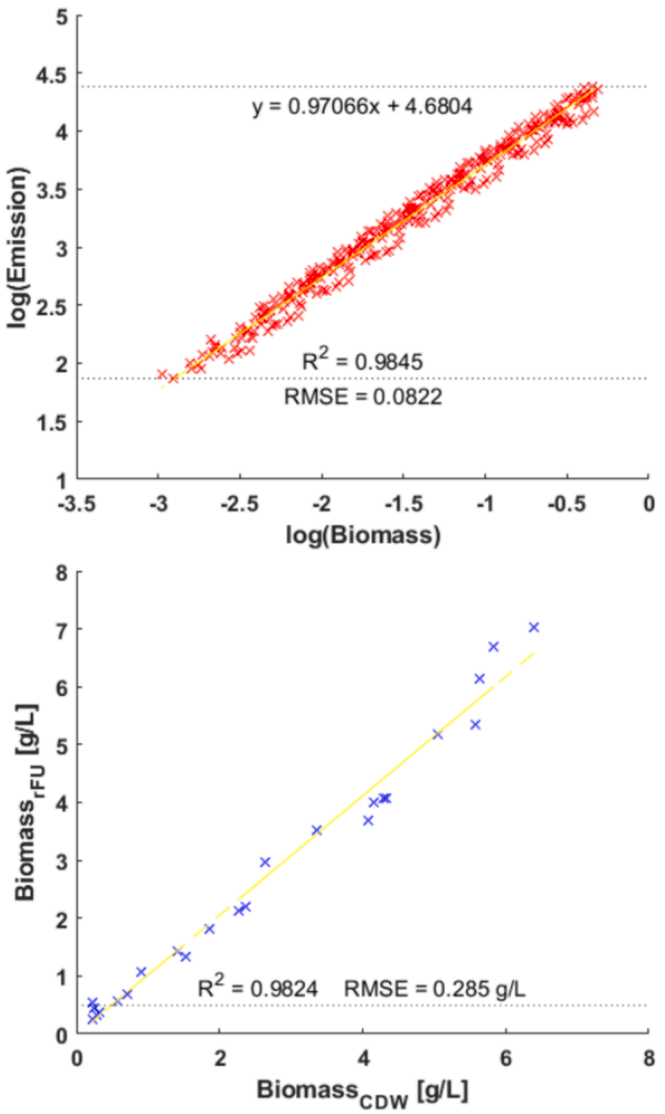

Fig. A.2. Tryptophan-based biomass measurement for *C. glutamicum* by fluorescence (Ex: 280/15 nm; Em: 340/20 nm). For the calibration set (42 samples), biomass concentration was plotted against emission in a double logarithmic plot (top) as proposed by Zabriskie and Humphrey (1978), resulting in 314 individual measurements within the linear range [1.87–4.38]. 24 independent samples were prepared as a test set and their measured cell dry weight was compared to the predictions of the fluorescence based measurement for method vali.dation (bottom).

under the applied conditions), which resulted in a lag phase of ≃ 16 h on 25 % UF-SSL. Increasing the starting target biomass concentration to 1 g/L shortened the lag phase to ⩽1 h. However, an increase to 1.5 g/L starting biomass concentration did not further shorten the lag phase or increase the substrate to biomass yields. Thus, increasing the biomass concentrations had diminishing returns once the lag phase was ≃ 1 h. Increasing the UF-SSL concentration from 25 % to 30 %, for 1 g/L starting biomass, again increased the lag phase from ⩽1 h to ≃ 12 h. Additionally, increasing the starting biomass concentration to 1.5 g/L decreased the lag phase to ≃ 6 h. In summary, an optimal combination of starting values must result in no significant formation of overflow metabolites and no significant lag phase (⩽1 h) in order to have optimal biomass per substrate yields. Increasingly higher initial biomass concentrations are required to achieve such a result as SSL % is increased, for example significantly more inoculum was required to achieve no lag phase for 30 % UF-SSL compared to 25 %. Therefore, a combination of 25 % UF-SSL with 1 g/L starting biomass was found to be optimal for batch start. However, this test revealed an additional challenge as the dry mass (after centrifugation and drying) was strongly correlated with the added NP feed (see supplementary material) resulting in a precipitate with stochastic particle size distribution (not simply removable by filtration or dissolving). Hence, the dry mass, which is commonly used as for determination of the cell dry weight (CDW) in biotechnology, could not be used as biomass measurement as an additional component, the precipitate, had an impact on the total dry mass.

3.2. Biomass quantification

In order to measure biomass within the complex matrix of UF-SSL, a variety of techniques were tested, which were, however, negatively affected by one of the following: precipitate weight (cell dry weight), precipitate absorption (optical density, total cell density probes), matrix effects (viable cell density probes, 2D fluorescence probes), cell clustering in the presence of inhibitors, such as furfural and HMF (lattice grid counting, automated cell counting, flow cytometry) and time constraints (colony forming units by plating & incubation). Examples of non-functional biomass measurement techniques are provided in the supplementary material with the most common *off-line* methods suffering from the inability to distinguish cells from precipitate particles. While *in-line* fluorescence-based methods were not directly applicable to UF-SSL due to the fluorescent background of the soluble lignin-derived compounds, these components (as opposed to the precipitate) can be removed by step-wise centrifugation, washing, and resuspension of the pellet. Hereby, measuring fluorescence of cellular tryptophan has been reported to be correlated to biomass concentration *in-line* by Zabriskie and Humphrey (1978), Horvath et al. (1993) and Surribas et al. (2006). After removal of the soluble lignin-derived components *off-line*, the measurement principle of fluorescence was unaffected by the remaining non-fluorescent precipitate particles. However, low biomass and precipitate concentrations are required to ensure that undesired reabsorption of the emitted light does not occur, although this is less of an issue *off-line* as sample dilution can be applied.

In order to establish such a cellular tryptophan-based biomass measurement for *C. glutamicum*, tests were performed with cells grown on yeast extract based medium. As described by Zabriskie and Humphrey (1978), biomass concentration versus emission was plotted in a double logarithmic graph. For the establishment of the calibration function, a serial dilution of 42 independent samples was performed on 96-well plates (11 dilutions + 1 blank per sample), of which 314 of 462 measurements fell within the ascertained liner range [1.87–4.38 log (Emission)]. Fig. A.2 shows the obtained linear correlation with a coefficient of determination R^2 of 0.985 distributed around the calibration curve with a root mean square error of 0.082. For validation, the CDW and fluorescence measurement results were plotted against each other, resulting in a linear correlation with a coefficient of determination R^2 of 0.982 and a root mean square error (RMSE) of 0.285 g/L for the independent test set. The main sources of uncertainty were the error of the reference measurement (CDW), the pellet washing and re-suspension, the serial dilution on 96-well plates and the error of the fluorescence measurement. For samples with a concentration of ⩽0.5 g/L biomass, the accuracy of the reference measurement (cell dry weight) decreased significantly. At the other end of the concentration range, higher biomass concentrations can be measured by pre-dilution of the samples. The developed method showed a high accuracy and precision as well as a large linear range and was therefore further used for evaluation of samples in the presence of UF-SSL. Method validation experiments testing for cellular tryptophan levels during growth on various C-sources and measurement reliability at the presence of precipitate (simulated by $CaSO_4$ addition) and UF-SSL in the sample matrix were performed (see supplementary material). However, the exact/realistic precipitate to biomass ratios were unknown and additional factors impacting the measurement in the presence of UF-SSL might occur. Therefore, method

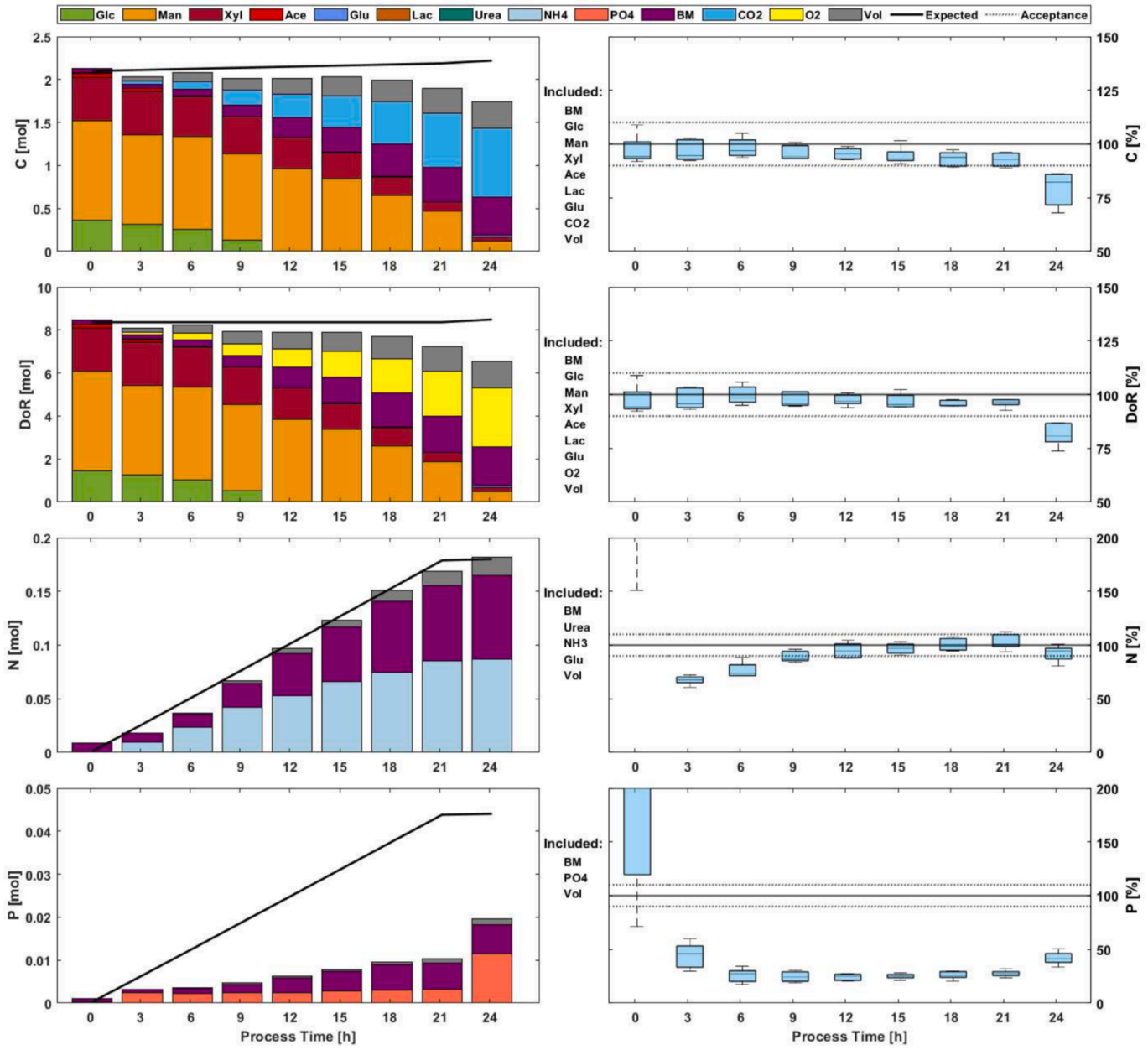

Fig. A.3. Elemental balances for a single process (left) and relative recovery for all 5 processes (right) for carbon (top most), DOR (top middle), phosphorus (bottom middle) and nitrogen (bottom most) during *C. glutamicum* cultivation's on UF-SSL. The amount added to the process (solid black line, left in mol, right as 100 % recovery) with an acceptance criteria of +/- 10 % over time (dotted lines) and samples (left as stacked bar chart, right as boxplot). For creation of the box plots all samples within +/- 5 min were pooled together and are represented as one box.

validation in the presence of UF-SSL was instead performed by analyzing the ability to close mass balances based on the biomass results obtained under actual process conditions, as described in the following sections, rather than with artificially created test cases.

Mass balances of C, N, P as well as the degree of reduction (DOR) were performed in order to: verify that all relevant C sources and sinks of *C. glutamicum* were accounted for and measured, check if N and P can be tracked throughout the process, analyze whether the obtained biomass values on SSL are reasonable in terms of allowing the closure of multiple mass balances at once and ensure data consistency and completeness (no further unknown components that affect the balances). The selection of analytes for balancing was performed to include only analytes that change significantly during the process, so as not to artificially inflate the absolute values, which would result in lower relative recoveries. For example, sugars that are not consumed by the cells (galactose, arabinose) were not included in the balances. Fig. A.3 shows the elemental balance of C, N, P and DOR for a single process as well as the relative recovery rate of all 5 processes. Acceptance criteria were set at +/- 10 % of relative recovery to account for measurement noise. All balances had initial measurements that met the expectations of the initial batch medium, although at the beginning of the process the relative errors of the N and P balances were elevated due to the absolute amounts being close to zero. Therefore, recovery rates for the first sample were calculated to be between 151–1409 % for N and 71–843 % for P. However, the recovery rate approaches 100 % and meets the acceptance criteria as the total N added to the system increases. For phosphorus, although the first sample was taken within minutes of inoculation and feed start, precipitation was present and increased with process time. This precipitation affected the P balance throughout the process. Attempts were made to include the precipitate in the P balance

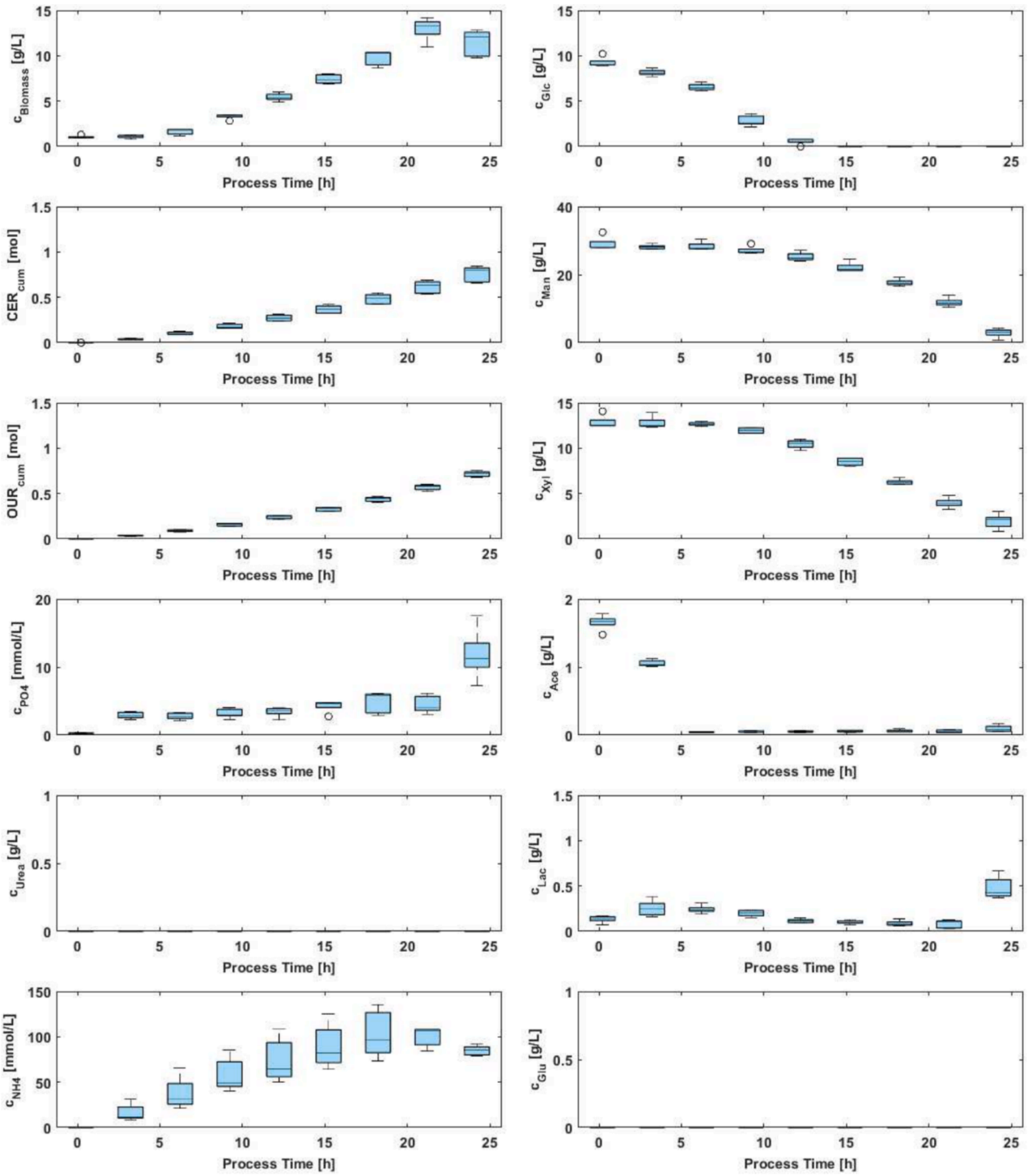

Fig. A.4. Box plots of the metabolite concentration over the course of 5 cultivation's of *C. glutamicum* on UF-SSL with the same conditions. For creation of the box plots all samples within +/- 5 min were pooled together and are represented as one box. For the boxes of CER and OUR the values were cumulated from the start of the cultivation up to the time point of the closest sample.

(data not shown), but these attempts were unsuccessful. The assumption that all of the precipitate was calcium phosphate ($Ca_3(PO_4)_2$) resulted in higher calculated concentrations of P than what was added to the process (even without consideration of other P-containing compounds). Furthermore, the formation of calcium phosphate in water is an extensively researched topic and highly complex (Nancollas et al., 1989) as it is affected by pH, temperature, Ca-P ratio as well as the presence of other ions and organic ligands to name a few, resulting in a variety of species ($Ca_3(PO_4)_2$, $Ca_8H_2(PO_4)_6{\cdot}5H_2O$, $CaHPO_4{\cdot}H_2O$ and more). To close the P balance for UF-SSL, accurate precipitate composition analysis (complicated by low solubility even in concentrated acids) proved necessary. The C & DOR balances had similar closing balances, albeit with slight underestimation at increasing process times. However, the total volume of liquid removed by sampling (interpolated and summed for each new sample based on the reactor weight) as well as the integration period of the online data from the off-gas analyzers increased with each subsequent sample. Hence, errors due to interpolation and integration accumulated, resulting in underestimation. The C and DoR balances met the

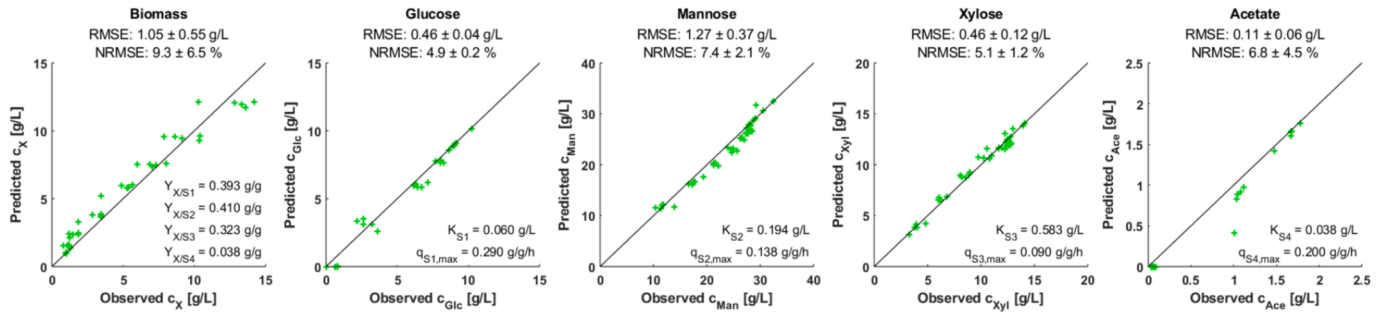

Fig. A.5. Observed concentrations (measurements) for all 5 batch cultivation's versus corresponding predicted concentrations (simulation) of the mechanistic process model. Ideal model fit is indicated by the 45° diagonal (black line), with the actual model fit for all samples from all experiments (green plus), with model parameter estimates shown in the respective plots. Furthermore, for each state [biomass (left), glucose (left middle), mannose (middle), xylose (right middle) and acetate (right)] RMSE and NRMSE were calculated including their standard deviation between the 5 processes. For normalization the difference between maximum and minimum state values was used for all states (modelling procedure taken from Sinner et al. (2019)).

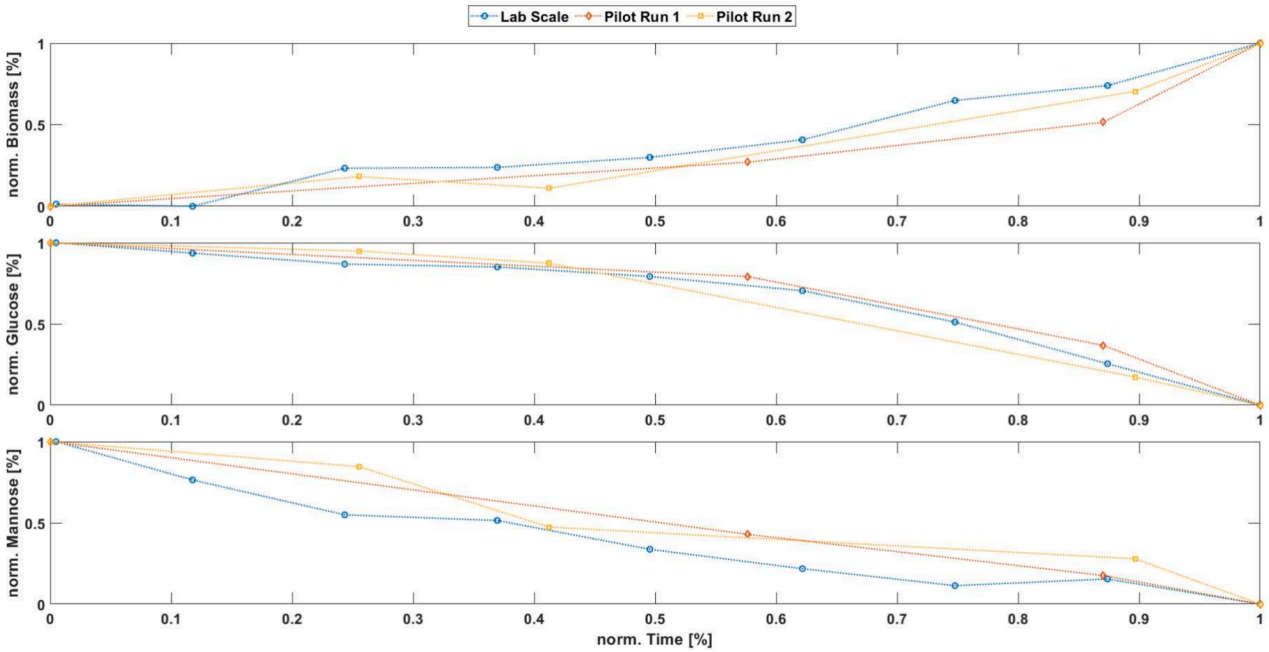

Fig. A.6. Scale comparison between 1 L *lab-scale* and 40 L *pilot-scale* batch cultivation's. Normalized concentration changes of biomass (top), glucose (middle) and mannose (bottom) were plotted against normalized time until glucose depletion.

acceptance criteria from the start up until ≃ 21 h. Afterwards, the batch phase was over and biomass started to decline, as will be discussed in more detail in the next section (Section 3.3), during which the spread between the biological replicates increased significantly. The loss of recovery during the biomass decline may be attributed to the washing of the pellet prior to fluorescence measurement (as cells begin to break down after cell death, pellet washing may remove smaller soluble cell fragments along with lignin-derived components). However, except for the sample at 24 h sample, the recovery was highly accurate considering the number of components tracked (with up to 8 different analytes plus sampling incorporated). The established calibration curve of cells grown on yeast extract based medium was applied to cells grown on UF-SSL based minimal medium, with 3 different balances based on first-principle successfully closing within +/- 10 %.

3.3. Reproducibility and kinetics

To ensure reproducibility, the developed batch cultivation was performed 5 times under the same conditions. Automated sampling was started after inoculation with an interval of 3 h, albeit slight offsets in sampling times between runs were present. Hence, for the generation of the box plots all samples within +/- 5 min of the intended sampling interval were pooled together and are represented as one box in the plots. Fig. A.4 displays the metabolite concentrations in the cultivation broth over time for all 5 batches. The selected combination of starting values resulted in no significant lag phase (⩽1 h) as well as no significant formation of overflow metabolites (lactate and glutamate) occurring. There was an exponential increase in biomass concentration up to the sample at 21 h, although there was a decrease in biomass concentration after 24 h. Notably, this decrease in biomass concentration was not reflected in CER or oxygen uptake rate (OUR) and did not coincide with a decrease in total substrate uptake rate across all C sources. However, an increase in lactate concentration coincided with the decrease in biomass, indicating a change in metabolism. Moreover, no correlation was found between trace element concentrations and biomass decline (data not shown). Of the 4 C sources in SSL, acetate and glucose were consumed initially with acetate being depleted after 5–6 h. After acetate depletion, mannose and xylose were starting to be consumed at low levels. However, once glucose was depleted after 9–10 h, the specific uptake rate of mannose and xylose increased significantly. All 4

Table A.1
Comparison of UF-SSL to a common defined medium for *C. glutamicum*.

Nutrients	CGXII	Keilhauer et al. (1993)	UF-SSL	Difference
Carbon Source				
Glucose	40 g/L		42 g/L [a]	105 %
Mannose	-		135 g/L [a]	–
Xylose	-		57 g/L [a]	–
Galactose	-		29 g/L [a]	–
Arabinose	-		13 g/L [a]	–
Acetate	-		6.4 g/L [b]	-
Nitrogen Source				
Ammonium	20 g/L	$(NH_4)_2SO_4$	⩽0.05 g/L [c]	⩽1 %
Urea	5 g/L		⩽0.025 g/L [a]	⩽1 %
TNb	-		0.28 g/L [d]	-
Phosphorus Source				
PO_4	1 g/L 1 g/L	KH_2PO_4 K_2HPO_4	0.05 g/L [e]	4 %
Trace Elements				
Magnesia	250 mg/L	$MgSO_4{\cdot}7H_2O$	350 mg/L [e]	1 419 %
Calcium	10 mg/L	$CaCl_2$	14 000 mg/L [e]	387 812 %
Iron	10 mg/L	$FeSO_4{\cdot}7H_2O$	23 mg/L [e]	1 150 %
Manganese	10 mg/L	$MnSO_4{\cdot}H_2O$	99 mg/L [e]	3 046 %
Zinc	1 mg/L	$ZnSO_4{\cdot}7H_2O$	9.7 mg/L [e]	4 133 %
Copper	0.2 mg/L	$CuSO_4$	⩽0.01 mg/L [e]	⩽13 %
Nickel	0.2 mg/L	$NiCl_2{\cdot}6H_2O$	0.32 mg/L [e]	648 %
Sodium	–		3 100 mg/L [e]	–
Additional Components				
Biotin	0.2 mg/L		–	–
Protocatechuic acid	30 mg/L		–	–
MOPS Buffer	42 g/L		–	–
Antibiotics	as required		–	–
Anti-foam	as required		–	–

[a] HPLC as described in Section 2.3
[b] Enzymatic Assay as described in Section 2.3
[c] DIN 38406 E5-1 (1983–10) A
[d] DIN EN 12260 H34 (2003–12) A
[e] DIN EN ISO 11885 (2009–09) A

substrates had a narrow spread throughout the cultivation, indicating consistent reproducible substrate uptake. Dissolved phosphate was present in low concentrations throughout the cultivation (≃ 5 mmol/L), providing a constant source of bioavailable phosphate for the cells. As enzymatic photometric assays are reported to be heavily impacted by cell lysis (Reichelt et al., 2016), it could not be excluded that the sudden increase in measured PO_4 at 24 h may be a result of the cell lysis. As the very first sample was taken shortly after inoculation and feed start, no significant amounts of NP-Feed were added to the reactor prior to sampling. Therefore, PO_4 and urea concentrations in the first sample were close to 0. Surprisingly, throughout the cultivation, all urea was immediately taken up by the cell and converted to ammonia and CO_2 by urease (Siewe et al., 1998). However, a small but increasing amount of ammonia built up in the broth over the course of the fermentation, indicating that nitrogen limitation was not occurring. Key performance indicators (KPI) of biomass growth rate $q_X(\mu)$ 0.102 +/- 0.041 h^{-1}, cumulative substrate uptake rate $q_{S_{cum}}$ 0.429 +/- 0.176 g/g/h and cumulative substrate to biomass yield $Y_{X/S_{cum}}$ 0.294 +/- 0.074 g/g were achieved.

Using the dataset with 5 processes parameter estimation of the Monod kinetics for glucose (S_1), mannose (S_2), xylose (S_3) and acetate (S_4) of the mechanistic model was performed according to Sinner et al. (2019). The model predictions with the estimated parameters compared to the actual concentrations of biomass, glucose, mannose, xylose and acetate can be seen in Fig. A.5. All states have relative errors of 5–10 %, which is within the acceptance criterion of ⩽10 % for a good model fit. For biomass, an overestimation was observed at low concentrations, whereas the highest observed values, which can be attributed to the last sample in each process, were underestimated. Hereby, it has to be mentioned that cell death was not considered in the model. However, with an RMSE of ≃ 1 g/L and normalised RMSE (NRMSE) of ≃ 9 %, the model to plant mismatch is acceptable, as the model error did not deviate significantly from the spread between the runs for higher biomass concentrations. Glucose, mannose and xylose all had a narrow spread between predictions which were close to the ideal, indicating high model accuracy. Similar results were observed for acetate, with only 1 point significantly deviating from the ideal prediction line, which may be attributed to reduced measurement accuracy at low concentrations (only samples at 0 h and 3 h had >0 g/L acetate) in the highly complex matrix of UF-SSL and was therefore considered an outlier. The genetic modification of the platform strain allowed for the consumption of xylose and an improved consumption of mannose compared to the wild-type. However, the estimated parameters indicated that glucose and acetate were still the preferred substrates of the platform strain. Glucose had the highest maximum specific uptake rate, followed by acetate and mannose and xylose with the lowest specific uptake rate, indicating that the used strain can take up significantly more glucose and acetate per time then mannose and xylose. Similarly, the affinity constants for glucose and acetate were significantly lower than those for mannose and xylose. Interestingly the biomass per substrate yield of mannose was the highest while glucose had only the second highest value and acetate had a significantly lower biomass per substrate yield than all other substrates. Since acetate and glucose were consumed before mannose and xylose, the degradation of inhibitory compounds of SSL might be the reason for the lower biomass yields (compared to defined medium without inhibitors), as some of the energy gained from metabolizing these substrates might be used to degrade inhibitors instead of growth.

3.4. Scale-up

In order to demonstrate that the proposed bioprocessing strategy can be transferred from *lab scale* to industrially relevant scales, two *pilot scale* runs were performed at Bio Base Europe Pilot Plant with kLA used as scale-up criterion. For comparison, normalized biomass, glucose and mannose concentration changes were plotted against normalized time until glucose depletion (Fig. A.6). Due to the low total amount of acetate (≃ 1.5 g/L in medium) and xylose (stronger carbon catabolite repression) consumed in the presence of glucose, their respective relative errors are overrepresented in double normalized plots ($\%_{ace}$ and $\%_{xyl}$ uptake over $\%_{time}$ until glucose depletion) and are therefore not shown separately. Furthermore, due to constraints at the pilot plant fewer samples were taken during the batch phase. Whereas the relative glucose uptake between *lab scale* and *pilot scale* showed no significant deviation, the initial biomass growth was increased. Although the same initial biomass target value was used at both scales, slightly higher actual initial biomass at *lab-scale* then in *pilot-scale* were measured (data not shown). As discussed in Section 3.1, the initial biomass concentration had key importance for biomass growth. Hence this slight deviation between scales in biomass growth may be attributed to the initial biomass. Correspondingly, the relative mannose consumption until glucose depletion was slightly higher in *lab-scale* than in *pilot-scale* since

relatively more biomass was present at that stage of the cultivation. Between scales relative KPI changes of 7% for $q_X(\mu)$, 9% for $q_{S_{1,2}}$ and 6% for Y_{X/S_1} occurred. As all KPI deviations were within the acceptance criteria of ⩽10%, they did not have a significant impact on the overall process and thus scale-up from *lab-scale* to *pilot-scale* was successful.

4. Conclusion

The main aim of this study was to develop a cheap, robust, quantifiable and scalable bioproduction platform based on SSL as alternative to production of ethanol with *S. cerevisiae*. Common simplifications, including the addition of expensive media components or energy/resource intensive detoxification steps, with low industrial relevance were entirely omitted. A minimal medium based on UF-SSL for a novel *C. glutamicum* strain was developed and a biomass quantification method tailored to the specific challenges of the substrate and cells was established and applied. Finally, process kinetics and robustness were assessed and a successful scale-up was done.

Declaration of Competing Interest

The authors declare that they have no known competing financial interests or personal relationships that could have appeared to influence the work reported in this paper.

Data availability

Uploaded to Mendely Data

Acknowledgments

This project has received funding from the Bio Based Industries Joint Undertaking under the European Union's Horizon 2020 research and innovation program under grant agreement No 790507 (iFermenter).

Appendix A

Figs. A.1–A.6 and Table A.1.

Appendix B. Supplementary material

Supplementary data associated with this article can be found, in the online version, at https://doi.org/10.1016/j.biortech.2024.130967.

References

Becker, J., Rohles, C.M., Wittmann, C., 2018. Metabolically engineered corynebacterium glutamicum for bio-based production of chemicals, fuels, materials, and healthcare products. Metab. Eng. 50, 122–141.

Brandt, B.A., García-Aparicio, M.P., Görgens, J.F., van Zyl, W.H., 2022. Adaptation of saccharomyces cerevisiae in a concentrated spent sulphite liquor waste stream for increased inhibitor resistance. Appl. Microbiol. Biotechnol. 1–14.

Cao, P., Christmann, J., Schwechheimer, S., Becker, J., Kohlstedt, M., Wittmann, C., Unpublished results. Utilization of spent sulphite liquor by corynebacterium glutamicum. Manuscript in preperation.

van Dijk, M., Erdei, B., Galbe, M., Nygård, Y., Olsson, L., 2019. Strain-dependent variance in short-term adaptation effects of two xylose-fermenting strains of saccharomyces cerevisiae. Bioresour. Technol. 292.

Fatehi, P., Ni, Y., 2011. Integrated forest biorefinery- sulfite process, in: Sustainable production of fuels, chemicals, and fibers from forest biomass. ACS Publications, pp. 409–441.

Guo, Z., Olsson, L., 2014. Characterization and fermentation of side streams from sulfite pulping. Process Biochem. 49, 1231–1237.

Han, X., Li, L., Bao, J., 2019. Microbial extraction of biotin from lignocellulose biomass and its application on glutamic acid production. Bioresour. Technol. 288, 121523.

Hassan, S.S., Williams, G.A., Jaiswal, A.K., 2019. Moving towards the second generation of lignocellulosic biorefineries in the eu. Renew. Sust. Energ. Rev. 101, 590–599.

Horvath, J.J., Glazier, S.A., Spangler, C.J., 1993. In situ fluorescence cell mass measurements of saccharomyces cerevisiae using cellular tryptophan. Biotechnol. Prog. 9, 666–670.

de Jong, E., Higson, A., Walsh, P., Wellisch, M., et al., 2012. Bio-based chemicals value added products from biorefineries. IEA Bioenergy, Task42 Biorefinery 34, 1–33.

Keilhauer, C., Eggeling, L., Sahm, H., 1993. Isoleucine synthesis in corynebacterium glutamicum. J. Bacteriol. 175, 5595–5603.

Kiefer, D., Merkel, M., Lilge, L., Hausmann, R., Henkel, M., 2021. High cell density cultivation of corynebacterium glutamicum on bio-based lignocellulosic acetate using ph-coupled online feeding control. Bioresour. Technol. 340, 125666.

Liu, Y.B., Long, M.X., Yin, Y.J., Si, M.R., Zhang, L., Lu, Z.Q., Wang, Y., Shen, X.H., 2013. Physiological roles of mycothiol in detoxification and tolerance to multiple poisonous chemicals in corynebacterium glutamicum. Arch. Microbiol 195, 419–429.

Morschett, H., Jansen, R., Neuendorf, C., Moch, M., Wiechert, W., Oldiges, M., 2020. Parallelized microscale fed-batch cultivation in online-monitored microtiter plates. J. Ind. Microbiol. Biotechnol. 47, 35–47.

Nancollas, G., LoRe, M., Perez, L., Richardson, C., Zawacki, S., 1989. Mineral phases of calcium phosphate. Anat. Rec. 224, 234–241.

Nigam, J., 2001. Ethanol production from hardwood spent sulfite liquor using an adapted strain of pichia stipitis. J. Ind. Microbiol. Biotechnol. 26.

Pereira, S.R., Sanchez i Nogue, V., Frazão, C.J., Serafim, L.S., Gorwa-Grauslund, M.F., Xavier, A.M., 2015. Adaptation of scheffersomyces stipitis to hardwood spent sulfite liquor by evolutionary engineering. Biotechnol. Biofuels. 8, 1–8.

Reichelt, W.N., Waldschitz, D., Herwig, C., Neutsch, L., 2016. Minimizing sample matrix effects for total protein quantification with bicinchoninic acid assay. J. Ind. Microbiol. Biotechnol. 43, 1271–1280.

Rødsrud, G., Lersch, M., Sjöde, A., 2012. History and future of world's most advanced biorefinery in operation. Biomass Bioenergy. 46, 46–59.

Rueda, C., Calvo, P.A., Moncalián, G., Ruiz, G., Coz, A., 2015. Biorefinery options to valorize the spent liquor from sulfite pulping. J. Chem. Technol. Biotechnol. 90, 2218–2226.

Sakai, S., Tsuchida, Y., Okino, S., Ichihashi, O., Kawaguchi, H., Watanabe, T., Inui, M., Yukawa, H., 2007. Effect of lignocellulose-derived inhibitors on growth of and ethanol production by growth-arrested corynebacterium glutamicum r. Appl. Environ. Microbiol. 73.

Shen, X.H., Zhou, N.Y., Liu, S.J., 2012. Degradation and assimilation of aromatic compounds by corynebacterium glutamicum. Appl. Microbiol. Biotechnol. 95, 77–89.

Siewe, R.M., Weil, B., Burkovski, A., Eggeling, L., Krämer, R., Jahns, T., 1998. Urea uptake and urease activity in corynebacterium glutamicum. Arch. Microbiol. 169, 411–416.

Sinner, P., Kager, J., Daume, S., Herwig, C., 2019. Model-based analysis and optimisation of a continuous corynebacterium glutamicum bioprocess utilizing lignocellulosic waste. IFAC-PapersOnLine 52, 181–186.

Sinner, P., Stiegler, M., Herwig, C., Kager, J., 2021. Noninvasive online monitoring of corynebacterium glutamicum fed-batch bioprocesses subject to spent sulfite liquor raw material uncertainty. Bioresour. Technol. 321.

Surribas, A., Montesinos, J.L., Valero, F.F., 2006. Biomass estimation using fluorescence measurements in pichia pastoris bioprocess. J. Chem. Technol. Biotechnol. 81, 23–28.

Tomás-Pejó, E., Olsson, L., 2015. Influence of the propagation strategy for obtaining robust s accharomyces cerevisiae cells that efficiently co-ferment xylose and glucose in lignocellulosic hydrolysates. Microb. Biotechnol. 8, 999–1005.

Tsuge, Y., Kudou, M., Kawaguchi, H., Ishii, J., Hasunuma, T., Kondo, A., 2016. Fudc, a protein primarily responsible for furfural detoxification in corynebacterium glutamicum. Appl. Microbiol. Biotechnol 100.

Unthan, S., Grünberger, A., van Ooyen, J., Gätgens, J., Heinrich, J., Paczia, N., Wiechert, W., Kohlheyer, D., Noack, S., 2014. Beyond growth rate 0.6: What drives corynebacterium glutamicum to higher growth rates in defined medium. Biotechnol. Bioeng 111, 359–371.

Xiros, C., Olsson, L., 2014. Comparison of strategies to overcome the inhibitory effects in high-gravity fermentation of lignocellulosic hydrolysates. Biomass Bioenergy 65, 79–90.

Yruela, I., 2005. Copper in plants. Braz. J. Plant Physiol. 17, 145–156.

Zabriskie, D., Humphrey, A., 1978. Estimation of fermentation biomass concentration by measuring culture fluorescence. Appl. Environ. Microbiol. 35, 337–343.